Short pulse multi-frequency phase-based time delay estimation

Said Assous,[a)] Clare Hopper, and Mike Lovell
Department of Geology, Ultrasound Research Laboratory, University of Leicester, Leicester LE1 7RH, United Kingdom

Dave Gunn, Peter Jackson, and John Rees
Ultrasound Research Laboratory British Geological Survey, Keyworth NG12 5GG, United Kingdom

(Received 6 January 2009; revised 9 October 2009; accepted 9 October 2009)

An approach for time delay estimation, based on phase difference detection, is presented. A multiple-frequency short continuous wave pulse is used to solve the well-known phase ambiguity problem when the maximum distance exceeds a full wavelength. Within an unambiguous range defined with the lowest frequency difference between components, the corresponding phase difference is unique and any distance within this range can be determined. Phase differences between higher frequency components are used to achieve a finer resolution. The concept will be presented and the effectiveness of the approach will be investigated through theoretical and practical examples. The method will be validated using underwater acoustic measurements, simulating noisy environments, demonstrating resolutions better than a 50th of a wavelength, even in the presence of high levels (−5 dB) of additive Gaussian noise. Furthermore, the algorithm is simple to use and can be easily implemented, being based on phase detection using the discrete Fourier transform.

I. INTRODUCTION

Time delay estimation is a fundamental step in source localization or beamforming applications and has attracted considerable research attention over the past few decades in many fields including radar, sonar, seismology, geophysics, ultrasonics, communication, and medical imaging. Various techniques are reported in the literature[1–5] and a state of the art review can be found in Ref. 6 which concerns critical techniques, limitations, and recent advances that have significantly improved the performance of time delay estimation in adverse environments. These techniques can be classified into two broad categories: correlator-based approaches and system-identification-based techniques. Both categories can be implemented using two or more sensors; in general, more sensors lead to increase robustness due to greater redundancy. When the time delay is not an integral multiple of the sampling rate, however, it is necessary to either increase the sampling rate or use interpolation.[6] In this paper, we present a new approach for time delay estimation, based on the received signal phase information. This avoids barriers encountered by alternative approaches based on phase information, which are limited by the need to use a reference signal, usually provided by a coherent local oscillator.[7] Ambiguities in such phase measurement, caused by the inability to count integer number of cycles (wavelengths), are resolved using the Chinese remainder theorem (CRT) taken from number theory, where wavelength selection is based on pair-wise relatively prime wavelengths.[7,8] However, the CRT is not entirely robust, in the sense that small errors in its remainders may induce a large error in the determined integer.[9,10] Another phase-based measurement approach, adopted to ensure accurate positioning of commercial robots, uses two or more frequencies in a decade scale in a transmitted signal. In this, the phase shift of the received signal with respect to the transmitted signal is exploited for ranging.[11,12] However, this approach is valid only when the maximum pathlength/displacement is less than one wavelength, otherwise a phase ambiguity will appear.

The time delay estimation approach proposed here is based on the use of local phase differences between specific frequency components of a short continuous wave (cw) received signal pulse. Within an unambiguous range defined by the lowest frequency difference between components, the corresponding phase difference is unique and any distance within this range can be determined. Phase differences between higher frequency components are used to achieve a finer resolution. Thus our approach overcomes the need to cross-correlate the received signal with either a reference signal or the transmitted signal. Unlike conventional methods, this approach is not limited by phase ambiguity; therefore most practical situations, where the range to be determined is beyond one wavelength, can be accommodated.

II. METHODOLOGY

A. Concept

The inspiration for development of the technique comes from the observation that bats have been shown to have exceptional resolution with regard to target detection when searching during flight.[13–15] Au and Simmons,[15] somewhat controversially, concluded that bats using pulses with a center frequency of about 80 kHz (40 kHz bandwidth) can achieve a distance resolution in air approaching 20 μm. At

[a)]Author to whom correspondence should be addressed. Electronic mail: sa251@le.ac.uk.

this frequency, and using $\lambda/2$ as the guide for resolution, we see that the resolution reported by Au and Simmons is about 200 times better than that predicted conventionally. We sought to develop a methodology which would allow us to approach a resolution comparable to that achieved by such creatures which is still better than any man-made system.

Consider an acoustic pulse containing a single frequency component f_1 with an initial zero phase offset. This pulse is emitted through the medium, impinges on a target, is reflected and returns. The signal is captured and its phase measured relative to the transmitted pulse. Given this situation, we cannot estimate the distance to and from an object greater than one wavelength away (hence, usually, we would estimate the time of arrival of the pulse and assume a value for the velocity of sound in the medium to estimate the distance to the target).

For simplicity, assume the pulse contains a single cycle of frequency f_1 of wavelength λ_1. The distance D to the target can be expressed as

$$D = n_1\lambda_1 + r_1, \tag{1}$$

where $\lambda_1 = v/f_1$, n_1 is an integer, r_1 is a fraction of the wavelength λ_1, and v is the speed of sound in the medium.

r_1 can be expressed as follows:

$$r_1 = \lambda_1 \times \frac{\phi_1}{360}, \tag{2}$$

where ϕ_1 is the residual phase angle in degrees. Combining Eqs. (1) and (2) and rearranging

$$D = n_1\lambda_1 + \lambda_1\frac{\phi_1}{360},$$

$$= n_1\frac{v}{f_1} + \frac{\phi_1}{360}\frac{v}{f_1},$$

$$D = \frac{v}{f_1}\left(n_1 + \frac{\phi_1}{360}\right). \tag{3}$$

If we transmit a second frequency component f_2 within the same pulse, then it will also have associated with it a wavelength λ_2 and a residual phase ϕ_2; similarly,

$$D = \frac{v}{f_2}\left(n_2 + \frac{\phi_2}{360}\right). \tag{4}$$

Equations (3) and (4) can be solved by finding Eq. (4) − Eq. (3) $\times(\lambda_2/\lambda_1)$ and rearranged to give

$$D = \left(\frac{\lambda_1\lambda_2}{\lambda_1 - \lambda_2}\right)\left((n_2 - n_1) + \frac{(\phi_2 - \phi_1)}{360}\right). \tag{5}$$

Using $v = f \times \lambda$, we obtain

$$D = \frac{v}{\Delta f}\left(\Delta n + \frac{\Delta\phi}{360}\right), \tag{6}$$

where $\Delta f = f_2 - f_1$, $\Delta n = n_2 - n_1$, and $\Delta\phi = \phi_2 - \phi_1$.

Knowing $D = v \times t$, we deduce the time delay t as

$$t = \frac{1}{\Delta f}\left(\Delta n + \frac{\Delta\phi}{360}\right). \tag{7}$$

If we impose the condition that $\Delta n \leqslant 1$, then Eq. (7) can be solved. This restriction on Δn is imposed as follows.

- A distance D is selected within which we require an unambiguous range measurement.
- Select a frequency f_1 within the bandwidth of the system, and its corresponding wavelength λ_1 [from Eq. (1)].
- Similarly, using Eq. (1), select frequency f_2 with its corresponding wavelength λ_2 such that the number of cycles is $n_2 = n_1 + 1$.

Considering Eq. (6), the maximum range is achieved by this approach when $\Delta n = 1$;

$$R = \frac{v}{\Delta f}. \tag{8}$$

Therefore, R is the maximum unambiguous range that can be achieved using the two frequencies f_1 and f_2 as described above. As the phase differences $\Delta\phi$ will be unique within this range R, any distance within this range can be determined unambiguously.

TABLE I. Parameters used in example 1.

R (mm)	v (mm/μs)	f_1 (kHz)	λ_2 (mm)	n_1	f_2 (kHz)	λ_2 (mm)	n_2
1500	1.50	200	7.50	200	201	7.462	201

B. Example

We demonstrate in this example how we could measure a range by using two frequencies and their related phase differences.

Consider an unambiguous range R; two frequencies f_1 and f_2 comprising integer number of cycles n_1, n_2 of wavelength λ_1, λ_2, respectively, as shown in Table I. Within this range R, consider a distance to target $d = 1000.1234$ mm we wish to estimate. Assume that a short cw pulse comprising these two frequencies f_1 and f_2 is sent toward the target at the distance d.

Using f_1, f_2 and Eqs. (1) and (6) for this distance d gives an integer number $n_1 = 133$ and a residual fraction of cycle of $r_1 = 0.349\,786$ corresponding to a residual phase of $\phi_1 = 125.923°$. Similarly for the frequency f_2, we find the residual phase $\phi_2 = 5.953°$ corresponding to $n_2 = 134$ and $r_2 = 0.016\,535\,6$. Thus, $\Delta\phi = \phi_2 - \phi_1 = -119.970°$.

We use this value in the formula given in Eq. (6), since $\Delta\phi$ is negative; this means $\Delta n = 1$. Using v from Table I, $\Delta f = 1$ kHz, and substituting into Eq. (7) give a first estimate of the range $\hat{d}_{f_1 f_2} = 1000.1233$ mm (caret is used here to mean an estimate). The unambiguous range R [Eq. (8)] is independent of the frequencies used depending only on the difference in frequency Δf.

TABLE II. Parameters used in example 2.

R (mm)	v (mm/μs)	f_3 (kHz)	λ_3 (mm)	n_3	f_4 (kHz)	λ_4 (mm)	n_4
1500	1.5	210	7.142	210	300	5.0	300

Note that in practice such resolution may not be achievable and limitations must be considered. For example, if the accuracy of estimating the phase is within $\pm 0.5°$, then the phases in the example above become $\phi_1 = 126.0$ and $\phi_2 = 6.0$, giving $d = 1000.0$ mm implying an error of 0.1234 mm. To get a finer resolution, we have to add other frequency components.

C. Using multiple frequencies through a "Vernier approach"

We demonstrate in this example how we could obtain a finer resolution in a range by using more than two frequencies and their related phase differences.

In Eq. (6), we imposed the condition that $\Delta n \leq 1$. The values of frequencies f_1 and f_2 were chosen to ensure this condition and to obtain a first estimate of the distance $\hat{d}_{f_1 f_2}$, and an estimate of the time delay $\hat{t}_{f_1 f_2}$ [Eq. (7)].

Introducing a third frequency f_3 as shown in Table II, such that $f_3 - f_1 = 10 \times (f_2 - f_1)$; f_2 differs from f_1 by 1 kHz and f_3 differs from f_1 by 10 kHz.

Again from Eq. (1), for f_3 and $d = 1000.1234$ mm, $\phi_3 = 6.219°$, which we would measure as 6.5°. Thus, $\Delta\phi_{13} = \phi_3 - \phi_1 = -119.5°$. We add 360° to give 240.5°. However, Δn_{13} between frequencies f_1 and f_3 is now 7 (in fact, 6 since we have already added in 360° to make the phase difference positive).

Using Eq. (6) with $\Delta\phi_{13}$ and different values of Δn_{13} (0–6) to get different distance estimate $\hat{d}^k_{f_1 f_3}$, where $k = 0, \ldots, 6$, in this case.

Applying Eq. (6) recursively for $\Delta n_{13} = 0, \ldots, 6$ to calculate $\hat{d}^k_{f_1 f_3}|_{k=0,6}$ selecting $\hat{d}^k_{f_1 f_3}$ closest in value to $\hat{d}_{f_1 f_2}$ as the optimum value $\hat{d}_{f_1 f_3} = 1000.2083 \text{ mm}|_{k=6}$. Hence, a new best time delay estimate $\hat{t}_{f_1 f_3|_{k=6}}$.

Note that the new best estimate distance is with an error of 0.0849 mm.

If a fourth frequency f_4 is introduced, as shown in Table II, such that the $\Delta f_{14} = 100.0$ kHz, using Eq. (1) again gives $\phi_4 = 8.8848°$ which we measure as 9°. Thus, $\Delta\phi_{14} = \phi_4 - \phi_1 = -117°$ which gives $\Delta\phi_{14} = 249.5$ after adding 360°. Note that $\Delta n_{14} = 66$ in this case.

Similarly, select the estimate $\hat{d}_{f_1 f_4}$ ($\Delta n = 0, 1, 2, \ldots, 66$) closest in value to $\hat{d}_{f_1 f_3}$. This occurs at $\Delta n_{14} = 66$ giving $\hat{d}_{f_1 f_4} = 1000.125$ mm. Taking this as the best estimate, the final error is 0.0016 mm = 1.6 μm.

Note that the frequencies need not be in decadal scale variation; however, they should be selected within the bandwidth of the system. All the selected frequencies should be a multiple of the lowest difference ensuring an integer number of cycles; in this way, we ensure that the phase calculated by the discrete Fourier transform (DFT) will be correct (i.e., corresponding exactly to the frequency bins). Thus, this example is reminiscent of the operation of a Vernier gauge as follows:

- $\Delta\phi_{12}$, related to the frequencies f_1 and f_2, gives the first estimate of the distance $\hat{d}_{f_1 f_2}$, hence $\hat{t}_{f_1 f_2}$.
- A higher frequency f_3 is then used (decade difference) to measure the same range but with a finer resolution. So a more accurate approximation to the measured range is obtained $\hat{d}_{f_1 f_3}$.
- Similarly, the measured range $\hat{d}_{f_1 f_4}$ corresponding to $\Delta\phi_{14}$ within f_1 and f_4, will give the ultimate estimate of the measured range d.
- Consequently, the maximum distance and the minimum resolution achieved are determined by the choice of the frequencies f_1, f_2, f_3, and f_4.

An example algorithm calculating the phase at each frequency and outlining the iterative phase difference measurements is given in the Appendix.

D. Phase offset measurement calibration

In the numerical example above, it is assumed that all phases are accurately transmitted and received, with no phase error on transmission or reception, and that all frequencies have zero phase offset with respect to each other. In practice this is almost certainly not the case and phase offsets between frequencies should be accounted for as discussed below.

Considering two frequencies $f_1 = 200.0$ kHz and $f_2 = 201$ kHz, and assuming the speed of sound in water ($v = 1.5$ mm/μs), from Eq. (8), the unambiguous range $R = 1500$ mm and Δn is 0 or 1. Considering the above

$$t = \frac{D}{v} = \frac{n + \phi/360}{f}. \tag{9}$$

Consider two distances d_1, d_2 corresponding to two "times" t_1 and t_2 such that the number of cycles n is the same for both frequencies over these distances, and assuming the phase measured includes a phase offset for that frequency. As an example, suppose the unknown phase offset for f_1 is 10°, for f_2 is 30°, and assume $d_1 = 100$ mm.

From Eq. (9), the term $(n_1 + \phi_1/360)$ would be calculated as 13.33 cycles, where $\phi_1 = 120°$. The "measured" $\phi_1 = 120 + 10 = 130°$ ($\phi_{1\text{measured}} = \phi_{1\text{distance}} + \phi_{1\text{offset}}$).

Similarly, for f_2 we obtain 13.40 cycles, where $\phi_2 = 144°$. The measured $\phi_2 = 144 + 30 = 174°$; from Eq. (7), $t_1 = 12.22$ μs. The actual time should be 6.66 μs.

Assume a second distance $d_2 = 200$ mm. Using Eq. (9), for f_1 we obtain 26.66 cycles, which gives $\phi_1 = 240°$. The measured $\phi_1 = 240 + 10 = 250°$. Similarly, for f_2 we obtain 26.80 cycles, which gives $\phi_2 = 288°$. The measured $\phi_2 = 288 + 30 = 318°$. Thus, using Eq. (7), $t_2 = 18.88$ μs. The actual time should be 13.33 μs.

A linear relationship could be deduced between t and d as follows:

$$t = m \times d + c, \tag{10}$$

where the slope $m=1/1.5=0.66$ is the speed of sound measured as 1 mm per 0.66 μs or $1/0.66=1.5$ mm/μs. The intercept $c=5.55$ μs is a measure of the relative phase between f_1 and f_2. Since $\Delta f_{12}=10$ kHz, 1 cycle is 100 μs long; consequently, the offset of 5.55 $\mu s \equiv 360\times(5.55/100)=20°$, which is equal to the relative phase (30–10) between the two frequencies. If we had known the phase offset between the two frequencies (20°), then in the calculation of times we would have obtained for t_1 a new phase difference of $(174-130-20)=24°$ giving a time for $t_1=6.66$ μs.

Similarly, for t_2 we obtain a new phase difference of $(318-250-20)=48°$ giving a time for $t_2=13.33$ μs. Both t_1 and t_2 are now correct. Note the following.

- If we assumed d_1 was 100 mm but it was actually, say, 120 mm and that d_2 was 200 mm but it was actually 220 mm, then we obtain the phase offset as 15.2°. The slope of Eq. (10) above, however, is unaffected. For example, such uncertainty may arise if the distance traveled by the wave within the transducers is not taken into consideration.
- If the temperature changes, so v changes; this changes the slope of Eq. (10) but not the time intercept or the phase offset. For example, if $v=1.6$ mm/μs, then equation Eq. (10) becomes $t=(1/1.6)\times d+5.55=0.625\times d+5.55$.

III. APPLICATION

A. Experiment

To demonstrate this approach, a series of measurements was performed in a water tank measuring $1530\times1380\times1000$ mm^3. Two broadband ultrasonic transducers (Alba Ltd., Glasgow, UK), having a wide bandwidth with a center frequency between 100 and 130 kHz, operate as both transmitters (Tx) and receivers (Rx) of ultrasound with a beam width of around 10° at the center frequency, where −3 dB bandwidth is 99 kHz (72−171 kHz). These were mounted on a trolley, movable in the X-Y directions. Linear encoders (Newall Ltd., Leicester, UK) were used to measure displacement of the rails in the x-direction and a software provided readouts of transducer positions. The temperature in the tank was measured by thermocouples calibrated using a quartz thermometers which are traceable to national standard. They were positioned on the four sides panels of the tank and recorded 19.80 ± 0.05 °C during the experiment. The experiment setup is shown in Fig. 1. The transmitter was driven by a 20 V peak-to-peak waveform consisting of short cw pulse comprising four frequencies (70, 71, 80, and 170 kHz). A modular system comprising a 16-bit arbitrary waveform generator (Ztec ZT530PXI) and a 16-bit digital storage oscilloscope (Ztec ZT410PXI) was used for transmit/receive process. Software was used to control signal transmission and acquisition. Distances between Tx and Rx of 305.800, 345.778, 481.128, 535.131, 535.252, 624.515, 759.182, and 862.887 mm were selected to be within an unambiguous range of $R\approx1500$ mm [Eq. (8)], as set by the linear encoders. A set of ten signals, noise free signal and signals with different signal to Gaussian noise ratios (SNR$=-20,-10,-5,-2,0,2,5,10,20$ dB), was transmitted at each distance described above. Note that the added Gaussian noise was generated by software and added to the original signal in each case. Before transmitting, each signal was multiplied by a Tukey window (cosine-tapered window with a 0.2 taper ratio) to reduce the "turn on" and "turn off" transients of the transducers. At each distance, three repeat pulses were transmitted and received for each SNR and each distance. Furthermore, 60 repeat pulses were transmitted and received while keeping the distance constant at 862.887 mm to assess the repeatability of the system (see Fig. 3). The sampling frequency F_s was set to 10 MHz, giving a number of samples $N=20000$ and a 2 ms pulse length. A DFT was then applied to the received pulses to obtain the magnitude and phase information for each of the four frequency components, using a window of $[N/2+1:N]$ for each received signal. This gave a resolution $F_s/N/2=1$ kHz which was consistent with the smallest step between the four frequencies comprised in the pulse.

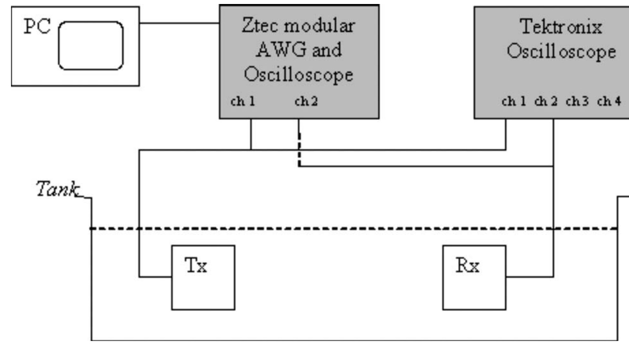

FIG. 1. Schematic diagram of the experimental setup.

Figure 2(a) shows the noise free transmitted (top) and received (bottom) signals when Tx and Rx were 305.800 mm apart, while Fig. 2(b) shows transmitted (top) and received (bottom) signal in the greatest noise case SNR (−20 dB). Note the DFT reports phase with respect to cosine, whereas sine waves were used in this experiment. Sine waves are returned with a phase of −90° relative to cosine waves by the DFT. This was not an issue, since relative phase differences were used. Using the phase for each distance obtained by the DFT, the phase-based time delay algorithm given in the Appendix was applied to obtain the corresponding estimated times for each phase difference $\Delta\phi_{12}$, $\Delta\phi_{13}$, $\Delta\phi_{14}$, $\Delta\phi_{23}$, $\Delta\phi_{24}$, and $\Delta\phi_{34}$, for the pairs f_1f_2, f_1f_3, f_1f_4, f_2f_3, f_2f_4, and f_3f_4, respectively.

Using a simple calculation of the first estimate by $t_{12}=\Delta\phi_{12}/(f_2-f_1)$ as a first estimate using Eq. (7) gave corresponding estimated times $\hat{t}_{12}$, $\hat{t}_{13}$, $\hat{t}_{14}$, $\hat{t}_{23}$, $\hat{t}_{24}$, and $\hat{t}_{34}$, respectively. For each distance, $\hat{t}_{14}$ should be the best estimate (i.e., the greatest Δf). The sensitivity of the algorithm to noise was reduced by the following.

- Limitation of the noise beyond the sensitivity of the transducer. The transducer act with its bandwidth as a bandpass filter.
- Signals were averaged 32 times during acquisition. When acquiring the signal with averaging, this reduces the noise level.
- The DFT operates on sine waves preferentially, even in the

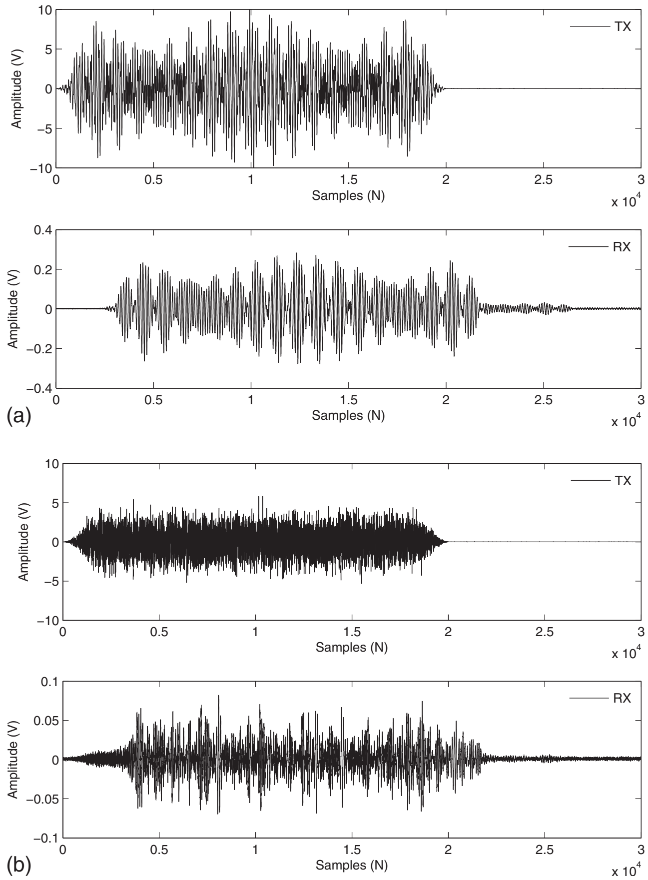

FIG. 2. Examples of transmitted and received short four components cw signals. Without (upper) and with (lower) added noise (−20 dB).

presence of noise. As the transmitted frequencies are known, when applying the DFT for the received signal, we will look just for those frequencies; hence any other frequencies are seen as noise and will not affect the frequencies of interest.

- Gradient estimation using a least squares fitting is noise tolerant. When doing the least squares estimation, any outlier which is basically noise will be removed.

B. Results and discussion

The best estimated time delays $\hat{t}_{14}$ for the eight different distances and using different signal-to-noise ratios are shown in Table III. For each distance, ten estimations were given corresponding to different signal-to-noise ratios. The column 2 corresponding to $\hat{t}_{14,Org}$, represents the estimated times when no noise was added to the signal. Using $\hat{t}_{14,Org}$ as best estimate time reference related to noise free signal, we can see that the technique became more robust to noise when the signal-to-noise ratio become greater than 2 dB. The variation is within 50, 30, 20, and 10 μs when the SNRs are 2, 5, 10, and 20 dB, respectively.

For the two rows in Table III corresponding to the distances 535.131 and 535.252 mm, where the displacement is about 120 μm, the estimated time for this displacement is about 120 ± 20 ns when the SNR is greater than −5 dB. As the sampling frequency used in this experiment was 10 MHz, using the conventional method (e.g., cross-correlation) to estimate the time delay, we would not get a best time resolution of less than $1/10^7 = 100$ ns, which corresponds to a displacement of 150 μm, when assuming a speed of sound of 1500 m/s. Hence, such displacement could not be measured without interpolation or oversampling. Moreover, if the cross-correlation approach was used to estimate the time delay in this experiment, all the measurements in Table III would be an integer of the sampling rate; in this case, 100 ns, as the technique is sampling-frequency dependent.

Figure 3(a) shows the time-distance plots, with the least squares fitting (linear regression), corresponding to the most noisy case (SNR=−20 dB). The error plot (bottom) shows the residuals with a norm of about 170 μs. Figure 3(b) shows the case of the best SNR (20 dB) and the corresponding residual error norm equal to 0.268 μs. The estimated time shown in y-axis corresponds to the best estimate $\hat{t_{14}}$ which is based on the phase difference between the two components $f_1 = 70$ kHz and $f_4 = 170$ kHz. The time delay estimation values with and without SNR ratios can be seen to be almost identical for each distance except for the two lowest SNR −20 and −10 dB. The data plotted in Fig. 3(b) (top) corresponds to a linear equations of the form $t = md + c$, where c is a measure of the phase offset for the two frequencies equal to $c \times (f_4 - f_1) \times 360$ and $1/m = v$ (mm/μs) is the estimated sound velocity in water, where m is the slope. Solving $t = md + c$ by least squares fitting gave the best estimate m, where $(1/m)$ is the speed of sound v in water.

Table IV represents the results after a least squares fitting estimation, showing the estimated sound velocity and the related offset for each situation (original and −20–20 dB

TABLE III. The estimated time delays for the eight distances with different SNR in Rx.

Distance (mm)	Estimated time (μs)									
d_{meas}	$\hat{t}_{14,Org}$	$\hat{t}_{14,-20\text{ dB}}$	$\hat{t}_{14,-10\text{ dB}}$	$\hat{t}_{14,-5\text{ dB}}$	$\hat{t}_{14,-2\text{ dB}}$	$\hat{t}_{14,0\text{ dB}}$	$\hat{t}_{14,2\text{ dB}}$	$\hat{t}_{14,5\text{ dB}}$	$\hat{t}_{14,10\text{ dB}}$	$\hat{t}_{14,20\text{ dB}}$
305.800	242.05714	328.14350	241.40850	241.86129	241.95502	241.99356	242.01367	242.03214	242.04162	242.04872
345.778	269.18036	366.64520	268.79819	269.06062	269.12812	269.14930	269.16954	269.17011	269.18868	269.18072
481.128	360.43477	347.04536	360.06666	360.31378	360.37864	360.39371	360.41009	360.40717	360.42855	360.43632
535.131	396.63307	492.90101	396.20888	396.50459	396.56616	396.59312	396.60089	396.62446	396.63076	396.62781
535.252	396.76493	493.05600	396.31506	396.62782	396.69481	396.73015	396.72628	396.73571	396.75997	396.75431
624.515	456.86671	442.81417	456.07791	456.61695	456.74634	456.78030	456.81829	456.82773	456.84870	456.85793
759.182	547.80206	522.71162	537.17804	547.60860	547.70913	547.73865	547.75749	547.78524	547.79431	547.80029
862.887	617.79228	391.21736	607.22052	617.63769	617.70199	617.72574	617.75122	617.78719	617.78503	617.80452

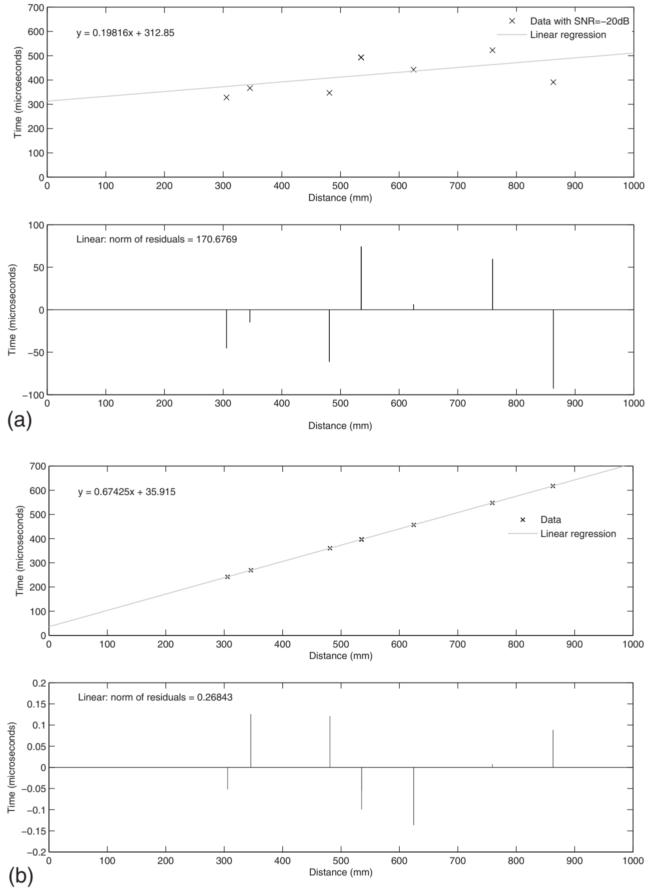

FIG. 3. Estimated times versus distances, −20 dB SNR case (top), noise free case (bottom), and their corresponding least squares fitting showing the residual errors.

SNR). The speed of sound is estimated to be 1483 m/s ± 0.2 m/s when the SNR is greater or equal to −5 dB and an average of temperature in the tank of 19.87 °C.

The speed of sound in pure water with similar temperature was reported in Ref. 16 to be 1481.727 m/s and in Ref. 17 to be 1482.36 m/s. Figure 4 shows the speed of sound variation versus different SNR ratios in a logarithmic scale; the approach can be seen to be less sensitive to noise when the SNR is greater than −10 dB.

Table V shows the measured distances and the corresponding estimated distances using the equations of Table

TABLE IV. Least squares fitting equations for different SNR in Rx and the corresponding estimated speed of sound from the slope.

Curve (dB)	$t=md+C$	$\hat{v}$ (mm/μs)	Phase offset
Noise free	$t=0.674\,182\times d+35.901\,766$	1.483 279	212.463 589
−20	$t=0.198\,160\times d+312.848\,259$	5.046 422	102.537 332
−10	$t=0.653\,855\times d+44.229\,354$	1.529 392	152.256 749
−5	$t=0.674\,171\times d+35.798\,682$	1.483 303	208.752 539
−2	$t=0.674\,186\times d+35.871\,635$	1.483 270	211.378 847
0	$t=0.674\,182\times d+35.901\,766$	1.483 279	212.463 589
2	$t=0.674\,197\times d+35.911\,676$	1.483 247	212.820 339
5	$t=0.674\,244\times d+35.900\,430$	1.483 142	212.415 469
10	$t=0.674\,221\times d+35.926\,900$	1.483 193	213.368 412
20	$t=0.674\,250\times d+35.914\,968$	1.483 130	212.938 860

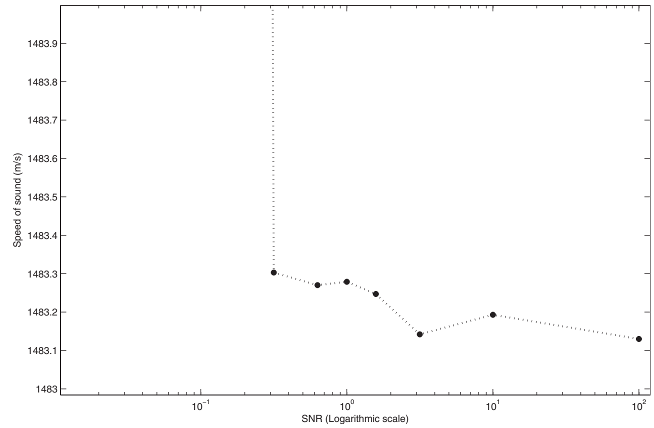

FIG. 4. Estimated speed of sound versus different SNRs (SNR= −5 to 20 dB).

IV. In this case, the estimated distance is given by $\hat{d}=(t-c)\times v$, where t is the estimated time corresponding to the best estimate $\hat{t_{14}}$, c is the time offset due to the time delay through the transducers, and v is the estimated sound velocity in water. The differences between the measured and estimated distances lie within the range 5–315 μm (see Table V) when the SNR is greater than −10 dB. The maximum difference represents 1/50 of the wavelength at the central frequency of the transducer (100 kHz).

IV. CONCLUSION

In this paper, a time delay estimation approach based on phase differences between components of the received short cw pulse signal is demonstrated. A validation underwater experiment showed that a resolution greater than 1/50 of the wavelength was achievable. Using local phase difference information, no ambiguity in phase measurement arises; hence there is no need to use the Chinese remainder theorem or a coherent local oscillator to overcome the wellknown phase ambiguity problem. As phase information is usually regarded to be useless in most correlator-based techniques, the approach developed in this paper is distinctive. Compared to correlator-based approaches, which have an estimation accuracy on the order of the used bandwidth, the suggested approach is not limited by the bandwidth but only by the ability to measure phase differences accurately. This leads to much improved performance once the SNR is sufficiently high. This approach is tolerant to additive Gaussian noise when the SNR is acceptable. Consequently, the technique offers the potential to outperform animals in subwavelength measurements. Although a bat can achieve a resolution of 20 μm in air,[15] potentially we would get a resolution of 4 mm/360 $=11$ μm. As a new approach, we expect that the algorithm will be improved to the point where one degree of phase can be resolved, suggesting that performance similar to the bat will be achieved by such technology in the near future.

ACKNOWLEDGMENTS

This work was undertaken as part of the Biologically Inspired Acoustic Systems (BIAS) project, funded by the RCUK Basic Technology Programme Grant Number EP/

TABLE V. The measured (using the encoders) and the estimated distances with different SNR in Rx.

Measured (mm) d_{meas}	Estimated distances (mm)									
	$\hat{d}_{org}$	$\hat{d}_{-20\ \mathrm{dB}}$	$\hat{d}_{-10\ \mathrm{dB}}$	$\hat{d}_{-5\ \mathrm{dB}}$	$\hat{d}_{-2\ \mathrm{dB}}$	$\hat{d}_{0\ \mathrm{dB}}$	$\hat{d}_{2\ \mathrm{dB}}$	$\hat{d}_{5\ \mathrm{dB}}$	$\hat{d}_{10\ \mathrm{dB}}$	$\hat{d}_{20\ \mathrm{dB}}$
305.800	305.785	77.186	301.564	305.653	305.677	305.691	305.700	305.722	305.707	305.723
345.778	346.017	271.482	343.453	345.998	345.982	345.971	345.979	345.972	345.972	345.963
481.128	481.372	172.573	483.039	481.354	481.331	481.312	481.311	481.289	481.298	481.307
535.131	535.065	908.622	538.314	535.036	535.007	535.005	534.991	535.004	534.993	534.984
535.252	535.260	909.404	538.477	535.218	535.198	535.209	535.177	535.169	535.185	535.171
624.515	624.408	655.862	629.877	624.200	624.270	624.280	624.308	624.294	624.308	624.313
759.182	759.290	1059.059	753.911	759.169	759.193	759.196	759.193	759.197	759.198	759.192
862.887	863.105	395.483	861.034	863.043	863.011	863.007	863.011	863.020	863.007	863.017

C523776/1. The BIAS project involves collaboration between the British Geological Survey, Leicester University, Southampton University, Leeds University, Edinburgh University, and Strathclyde University. This paper is published with the permission of the Executive Director of the British Geological Survey (NERC).

APPENDIX: TIME DELAY ESTIMATION ALGORITHM USING PHASE DIFFERENCES

Input: Set of phases $(\phi_1, \phi_2, \phi_3, \phi_4)$ and frequencies (f_1, f_2, f_3, f_4)
Output: Set of estimated time delay $(\hat{t}_{12}, \hat{t}_{13}, \hat{t}_{14}, \hat{t}_{23}, \hat{t}_{24}, \hat{t}_{34})$
foreach *Received signal, k* **do**
  Calculate DFT (f_1, f_2, f_3, f_4, k);
  Get $\phi_1, \phi_2, \phi_3, \phi_4$
end
foreach $(i,j)=(1,3);(1,4);(2,3);(2,4);(3,4)$ **do**
  $\Delta\phi_{ij} = \phi_j - \phi_i$;
  if $((\Delta\phi_{ij}) < 0)$ **then**
    $\Delta\phi_{ij} = \Delta\phi_{ij} + 360.0$;
  end
end
$\Delta\phi_{12} = \frac{\Delta\phi_{12}}{360.0}$, $\Delta f_{12} = f_2 - f_1$, $\hat{t}_{12} = \frac{\Delta\phi_{12}}{\Delta f_{12}}$, $\hat{t}_{old} = \hat{t}_{12}$
foreach $(i,j)=(1,3);(1,4);(2,3);(2,4);(3,4)$ **do**
  if $((\hat{t}_{old} \times \Delta f_{ij}) < 1.0)$ **then**
    $\hat{t}_{new} = \frac{\Delta\phi_{ij}}{\Delta f_{ij}}$;
    nmin $= -1$;
  end
  $min 1.0e+06$;
  for each $n = 0$ *to* 1000 **do**
    Calculate $\hat{t}_{ij} = (n + \Delta\phi_{ij})/\Delta f_{ij}$;
    $\Delta t = |\hat{t}_{ij} - \hat{t}_{old}|$;
    if $(\Delta t < min)$ **then**
      $min = \Delta t$;
      $\hat{t}_{new} = \hat{t}_{ij}$;
      nmin $= n$;
    end
  end
end

[1] G. H. Knapp and G. C. Carter, "The generalised correlation method for estimation of time delay," IEEE Trans. Acoust., Speech, Signal Process. **24**, 320–327 (1976).
[2] G. C. Carter, "Time delay estimation for passive sonar signal processing," IEEE Trans. Acoust., Speech, Signal Process. **29**, 463–470 (1981).
[3] G. C. Carter, "Coherence and time delay estimation," in *Signal Processing Handbook*, edited by C. H. Chen (Dekker, New York, 1998), pp. 443–482.
[4] R. E. Boucher and J. C. Hassab, "Analysis of discrete implementation of generalised cross-correlator," IEEE Trans. Acoust., Speech, Signal Process. **ASSP-29**, 609–611 (1981).
[5] J. Chen, J. Benesty, and Y. A. Huang, "Time delay estimation via linear interpolation and cross correlation," IEEE Trans. Speech Audio Process. **12**, 509–519 (2004).
[6] J. Chen, J. Benesty, and Y. A. Huang, "Time delay estimation in room acoustic environments: An overview," EURASIP J. Appl. Signal Process. **2006**, 1–19.
[7] L. Belostotski, T. L. Landecker, and D. Routledge, "Distance measurement with phase stable CW radio link using the Chinese remainder theorem," Electron. Lett. **37**, 521–522 (2001).
[8] C. E. Towers, P. D. Towers, and D. C. Jones Julian, "The efficient Chinese remainder theorem algorithm for full-field fringe phase analysis in multi-wavelength interferometry," Opt. Express **12**, 1136–1143 (2004).
[9] X. Xiang-Gen and L. Kejing, "A generalized Chinese remainder theorem for residue sets with errors and its application in frequency determination from multiple sensors with low sampling rates," IEEE Signal Process. Lett. **12**, 768–771 (2005).
[10] O. Goldreich, D. Ron, and M. Sudan, "Chinese remaindering with errors," IEEE Trans. Inf. Theory **93**, 1330–1338 (2000).
[11] A. K. T. Lee, J. Lucas, and L. E. Virr, "Microcomputer-controlled acoustic rangefinding technique," J. Phys. E: J. Sci. Instrum. **22**, 52–58 (1989).
[12] M. Yang, S. L. Hill, B. Bury, and J. O. Gray, "A multifrequency AM-based ultrasonics system for accuracy distance measurement," IEEE Trans. Instrum. Meas. **43**, 861–866 (1994).
[13] H. Hartridge, "Acoustical control in the flight of bats," Nature (London) **156**, 490–494 (1945); **156**, 692–693 (1945).
[14] J. A. Simmons, "The resolution of target range by echolocating bats," J. Acoust. Soc. Am. **54**, 157–173 (1973).
[15] W. L. Whitlow and J. A. Simmons, "Echolocation in dolphins and bats," Phys. Today **60**(9), 40–45 (2007).
[16] V. A. Del Grosso and C. W. Mader, "Speed of sound in pure water," J. Acoust. Soc. Am. **52**, 1442–1446 (1972).
[17] N. Bilaniuk and G. S. K. Wong, "Speed of sound in pure water as a function of temperature," J. Acoust. Soc. Am. **93**, 1609–1612 (1993).